

Optimization of Heat Sink Design and Fan Selection in Portable Electronics Environment

Abstract

Modern portable electronics have seen component heat loads increasing, while the space available for heat dissipation has decreased, both factors working against the thermal designer. This requires that the thermal management system be optimized to attain the highest performance in the given space. While adding fins to the heat sink increases surface area, it also increases the pressure drop. This reduces the volumetric airflow, which also reduces the heat transfer coefficient. There exists a point at which the number of fins in a given area can be optimized to obtain the highest performance for a given fan. The primary goal of this paper is to find the optimization points for several different fan-heat sink designs. The secondary goal is to find a theoretical methodology that will accurately predict the optimization point and the expected performance.

Key Words: thermal resistance, gap/length ratio, pressure drop, optimization and fan-heat sink system.

Nomenclature

A_d	Duct cross sectional area, mm^2
A_b	Heat sink base area, mm^2
A_f	Fin surface area, mm^2
A_m	Fin profile area, mm^2
A_{sc}	Heat source contact area, mm^2
D_h	Hydraulic Diameter, mm
f	Friction factor
f_{app}	Apparent friction factor
g	Channel width, mm
h	Convection heat transfer coefficient, $\text{W}/\text{m}^2\text{K}$
h_f	Fin height, mm
k_{air}	Air thermal conductivity, W/mK
k_m	Material thermal conductivity, W/mK
K_c	Contraction coefficient
K_{cd}	Duct Contraction Coefficient
K_e	Expansion coefficient
K_{ed}	Duct Expansion Coefficient
L	Fin length, mm
L_c	Corrected length, mm
Nu_g	Nusselt number
P	Total input power, W
Pr	Prandtl Number
Re_{Dh}	Hydraulic Diameter Reynolds Number
Re_g	Channel Reynolds number
Re_a^*	Approach velocity Reynolds number
T_{amb}	Ambient temperature, $^{\circ}\text{C}$
T_b	Heat sink base temperature, $^{\circ}\text{C}$
t	Fin thickness, mm
t_b	Heat sink base thickness, mm
w	Fin pitch, mm
x_l	Channel length, mm
x^+	Dimensionless hydrodynamic entry length
V_g	Channel velocity, m/s

V_{fs}	Free stream velocity, m/s
V_a	Actual approach velocity, m/s
ΔP	Heat sink pressure drop, N/m^2
ΔP_{th}	Theoretical Heat sink pressure drop, N/m^2
λ	Spreading resistance variable, m^{-1}
η_f	Fin efficiency
ρ	Fluid density, Kg/m^3
ν	Fluid viscosity, m^2/s
Θ_{ave}	Average heat sink thermal resistance, $^{\circ}\text{C}/\text{W}$
Θ_{ba}	Experimental thermal resistance, $^{\circ}\text{C}/\text{W}$
Θ_f	Fin thermal resistance, $^{\circ}\text{C}/\text{W}$
Θ_s	Base spreading resistance, $^{\circ}\text{C}/\text{W}$
Θ_t	Total resistance, $^{\circ}\text{C}/\text{W}$

Introduction

Rapid development in packaging technology allows portable electronics to gain faster processing speed and enhanced capabilities. However, thermal management in the portable electronics environment is becoming increasingly difficult due to high heat load and dimensional constraints. Proper selection of fans and fin pitch in the heat sink is crucial to ensure the thermal design of the system is optimized.

Figures 1 and 2 show the common thermal solutions found in today's portable computer environment. The micro blower-heat sink heat pipe assembly shown in Figure 1 is mounted on a slim cold plate. Heat pipes transport the heat generated by the chip, where it is dissipated to the environment with the aid of the airflow produced by the micro blower. This type of thermal design is deployed in a system with limited space. The fin designs are optimized to assure maximum heat transfer occurs between the fins and the surrounding ambient. The micro blower is capable of supplying sufficient airflow to cool the system while maintaining a low profile to fulfill the space restriction [1]. The axial fan-heat pipe-heat sink assembly shown in Figure 2 is used when space is less constrictive. A heat pipe transports heat from the source to the high efficiency fins enclosed in a square block with an axial fan attached at one end to pull airflow through the fins.

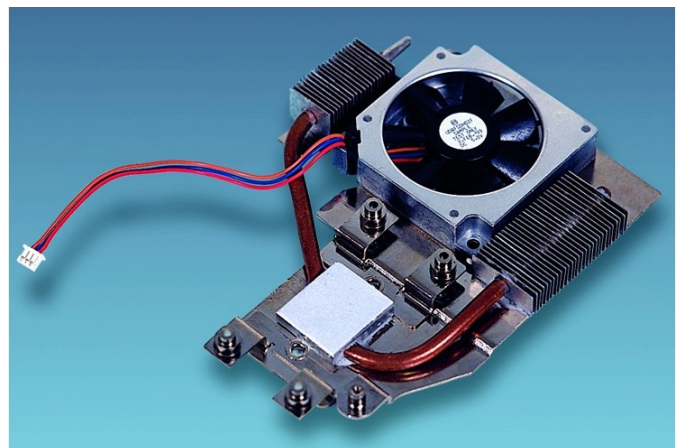


Figure 1: Micro blower-heat sink system for portable computer.

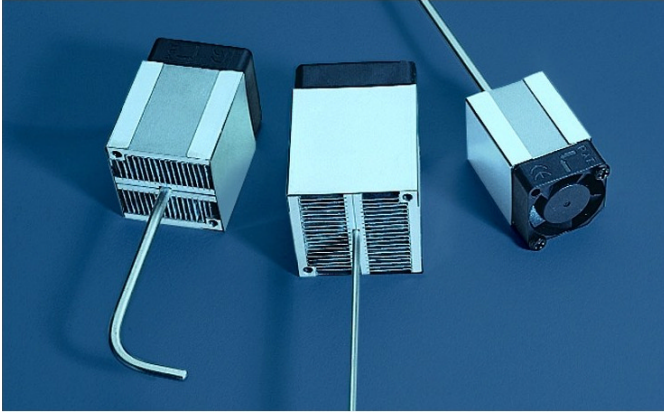


Figure 2: Axial fan-heat sinks systems for portable computer.

The main objective of this paper is to investigate the effects on thermal performance under axial fan and micro blower airflow for different gap/length ratio heat sinks. In doing so, the optimization point between the different types of fans or blowers under certain fin gap/length ratio can be obtained. In addition, the experimental results are used to compare with theoretical methodology developed by Copeland [2], Biber [3], and Teertstra [4].

Analytical Model

A fan-heat sink model can be characterized based on the following assumptions:

- No flow bypassing since the heat sink is fully ducted
- Isotropic material
- Fin tips are adiabatic
- Uniform approach velocity

This model can be further broken down into two sections, the calculation of pressure drop across the heat sink and finding the overall thermal resistance of the heat sink.

Total Heat Sink Pressure Drop

The accelerating flows inside the heat sink channel produces a pressure drop between the channel entrance and exit region. This pressure drop across the heat sink is also known as the system resistance. System resistance affects the overall thermal performance of heat sink. Higher system resistance causes less airflow through the heat sink channel, attaining lower convection heat transfer rate between the fins and the surrounding air and increases the fin thermal resistance. When the heat sink system resistance is known, the actual volumetric flow rate can be found from the fan/blower performance curve with a given total heat sink pressure drop. This point along the fan/blower curve is called the system operating point.

The system operating point shifts up and down along the performance curve depending on the constraints (hydrodynamic head, geometry of heat sink and fluid properties) imposed upon the system [5]. When the fan performance is balanced by the system performance to deliver the most efficient combination of airflow and heat sink surface area. The system is said to be optimized at that operating point.

To evaluate the total pressure drop across the heat sink, we must first determine the hydraulic diameter and channel velocity. They are given as follows:

$$D_h = \frac{2gh_f}{g + h_f} \quad (1)$$

$$V_g = V_{fs} \left(1 + \frac{t}{g} \right) \quad (2)$$

The channel velocity is related to the free stream velocity and the ratio of fin thickness and the channel width. Using these variables with fluid properties, the Reynolds number is found to be:

$$Re_g = \frac{D_h V_g}{\nu} \quad (3)$$

Generally, the velocity profile in the heat sink channel is laminar, in which the Reynolds number is below 2300. Also, in most cases, the channel length is not long enough for the flow in the channel to become fully developed, and hence, the flow is a mixture of fully developed and developing flow. The apparent friction factor for this mixture of flow is a function of friction factor of the fully developed flow and the hydrodynamic entrance length. The approximate equation is taken from Shah and London [6]:

$$f_{app} Re_g = \left[\left\{ \frac{3.2}{(x^+)^{0.57}} \right\}^2 + \{f Re_g\}^2 \right]^{1/2} \quad (4)$$

The fully developed flow friction factor, $f Re_g$, is obtained from Kays and London [7]. Since the flow is laminar, the dimensionless hydrodynamic entrance length is defined as a function of Reynolds number, hydraulic diameter and the length of the channel as follows [8]:

$$x^+ = \left(\frac{x_1}{Re_{D_h} D_h} \right)_{laminar} \quad (5)$$

The laminar flow contraction and expansion loss coefficients are defined as [2]:

$$K_c = 0.8 - 0.4(g/w)^2 \quad (6)$$

$$K_e = [1 - (g/w)]^2 - 0.4(g/w) \quad (7)$$

The total heat sink pressure drop is formulated as:

$$\Delta P = (K_c + 4f_{app} x^+ + K_e) \cdot \left(\frac{\rho V_g^2}{2} \right) \quad (8)$$

For our case, we added the contraction and expansion loss coefficients of the duct to closely represent the experiment. These coefficients are found in Munson, Young and Okiishi [9]. Therefore, the total heat sink pressure drop equation (8) becomes:

$$\Delta P_{th} = (K_c + K_{ed} + 4f_{app}x^+ + K_e + K_{ed}) \cdot \left(\frac{\rho V_g^2}{2} \right) \quad (9)$$

The theoretical total heat sink pressure drop can be inserted into any commercially available fan performance curve to determine the volumetric flow rate at that given point. The actual approach velocity can be calculated by dividing the volumetric flow rate with duct cross sectional area.

$$V_a = \text{Volumetric Flow Rate}/A_d \quad (10)$$

The newly found approach velocity is then used to compute the heat sink thermal resistance.

Total Thermal Resistance

The total thermal resistance is the product of the fin thermal resistance and the base spreading resistance, expressed as follow:

$$\Theta_t = \Theta_f + \Theta_s \quad (11)$$

Fin Thermal Resistance

With the adiabatic fin tip assumption, the fin thermal resistance is given by:

$$\Theta_f = \frac{1}{\eta_f A_f h} \quad (12)$$

In order to compute the coefficient of heat transfer, h , the approach velocity Reynolds number, Re_a^* , must be calculated first. The approach velocity Reynolds number is evaluated by taking the aspect ratio of the channel width to length and it is defined as:

$$Re_a^* = \frac{V_a g}{\nu} \left(\frac{g}{L} \right) \quad (13)$$

Since the channel flow is partly fully developed and developing flow, the composite model proposed by Teertsra is used to calculate the average Nusselt number in the channel [4]:

$$Nu_g = \left[\left(\frac{Re_a^* Pr}{2} \right)^{-3} + \left(0.664 \sqrt{Re_a^*} Pr^{\frac{1}{3}} \sqrt{1 + \frac{3.65}{\sqrt{Re_a^*}}} \right)^{-3} \right]^{\frac{1}{3}} \quad (14)$$

Using the above approximation, the coefficient of heat transfer, h , can be expressed as:

$$h = \frac{Nu_g k_{air}}{L} \quad (15)$$

With the assumption that the fin width is sufficiently large compared with the fin thickness, and along with the coefficient of heat transfer and fin geometry, the fin efficiency, η_f , is given as [10]:

$$\eta_f = \frac{\tanh mL_c}{mL_c} \quad (16)$$

where mL_c is defined as:

$$mL_c = \sqrt{\frac{2h}{k_m A_m}} L_c^{\frac{3}{2}} \quad (17)$$

and the corrected fin length and fin profile area are found using these equations:

$$L_c = L + \frac{t}{2} \quad (18)$$

$$A_m = L_c t \quad (19)$$

Base Spreading Resistance

As heat flows across the cross sectional area of the base, it encounters resistance and therefore gives rise to the base temperature. Depending on the size of the heat source, the smaller the heat source, the higher the base spreading resistance. The empirical solution by Lee is shown as follows [11]:

$$\Theta_s = \left(\frac{\sqrt{A_b} - \sqrt{A_{sc}}}{k_m \sqrt{\pi A_b A_{sc}}} \right) \cdot \left(\frac{\lambda k_m A_b \Theta_{ave} + \tanh(\lambda t_b)}{1 + \lambda k_m A_b \Theta_{ave} \tanh(\lambda t_b)} \right) \quad (20)$$

where λ is given as:

$$\lambda = \frac{\pi^{\frac{3}{2}}}{\sqrt{A_b}} + \frac{1}{\sqrt{A_{sc}}} \quad (21)$$

In our study, the average thermal resistance, Θ_{ave} , is assumed to be equal to the fin thermal resistance, Θ_f .

Experimental Method

Figure 3 shows the test sample experimental setup. There are total of 8 heat sink samples with varying pitches. Three thermocouples are inserted into the pilot holes in the base to monitor the base temperature.

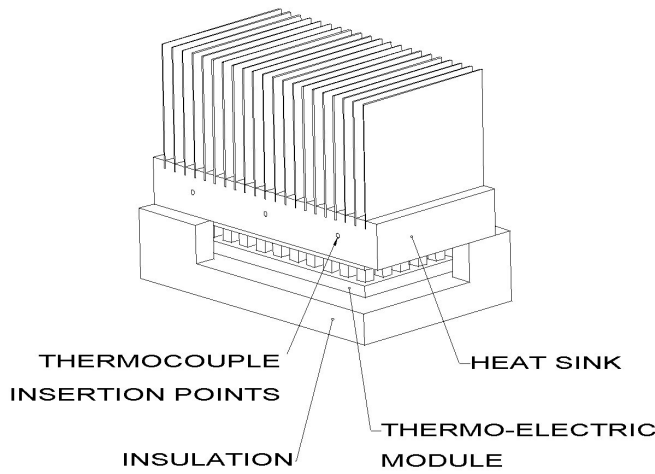


Figure 3. Experimental Setup of Test Sample

Thermal grease is used as an interface material between the heat source and heat sink base. The thermoelectric module serves as heat source in this experiment. The design specifications of heat sink sample are listed in Table 1.

Table 1. Heat Sink Sample Design Specifications

Fin Material	Aluminum A3003
Fin Thickness	0.2mm
Fin Pitch	0.95mm, 1.05mm, 1.20mm, 1.30mm, 1.45mm, 1.55mm, 1.70mm, 1.80mm
Base Material	Copper C110
Base Thickness	6mm
Overall Sample Dimension	20L x 40W x 20H mm

The wind tunnel assembly used for heat sink characterization is shown in Figure 4. The DC axial fan module is attached to one end of the wind tunnel to deliver airflow through the duct. The test sample in Figure 3 is mounted in the closely ducted test section of the wind tunnel. Temperature measurements taken from the base are output to the data logger for recording. The test samples are tested under 2 different DC axial fans with different volumetric flow rates and head pressure.

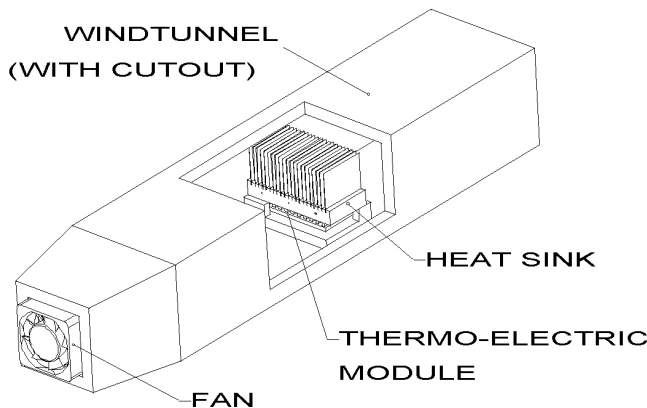


Figure 4. Schematic of Experimental Setup with Axial Fan

Figure 5 shows the wind tunnel assembly with micro blower attachment. The experimental procedures for micro blower are the same as the DC axial fan.

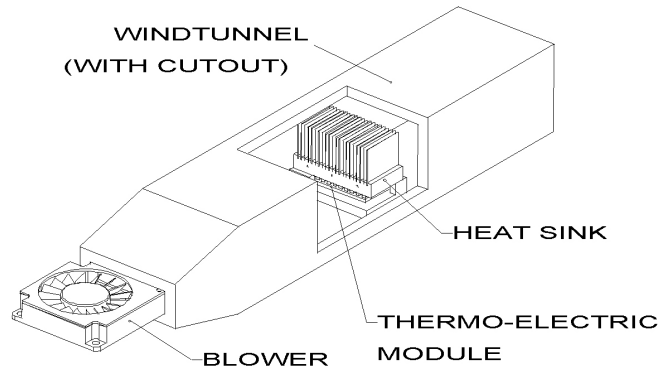


Figure 5. Schematic of Experimental Setup with Micro Blower

Table 2 provides the fans and blowers specification used in this experiment.

Table 2. Blowers and Fans Specifications

Type	Power (W)	Dimension (mm)	Max Flow Rate (CFM)	Max Static Pressure (mmH ₂ O)
High Power Blower	0.75	40 x 40 x 10	2.40	7.24
Low Power Blower	0.45	40 x 40 x 10	1.60	5.34
High Power Axial Fan	0.65	30 x 30 x 10	4.10	3.68
Low Power Axial Fan	0.30	30 x 30 x 10	1.99	1.48

The experimental thermal resistance, Θ_{ba} , is a measure of the temperature difference between the base and ambient air over the power delivered by the thermoelectric module. It is defined as:

$$\Theta_{ba} = \frac{T_b - T_{amb}}{P} \quad (22)$$

Discussion of Results

Figure 6 shows the experimental thermal resistances versus the channel width/length ratio for the 4 different fan types. It is observed that the low power blower has the worst thermal performance and the high power axial fan turned out to be the overall best performer. The high power blower performed nearly as well as the high power axial fan. Figure 6 also shows that the order of the fans performance matches the fans maximum volumetric flow rate.

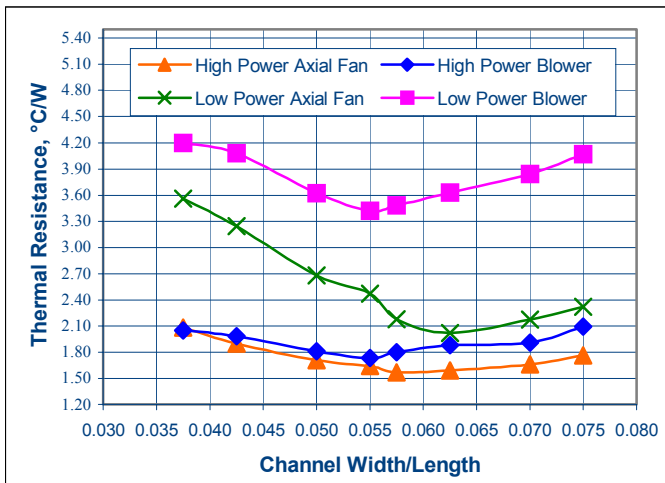


Figure 6. Experimental Total Thermal Resistance vs. The Channel Width/Length Ratios with different types of Micro Blower and Axial Fan

Comparing between the optimization points of the blowers and axial fans, both blowers produced a local minima at 0.055 width/length ratio. As for the high and low power axial fans, optimizations are found on the points of 0.0575 and 0.0625 width/length ratio respectively. This suggests that the mass flow rate of the axial fans is more greatly hindered by the pressure drop of the heat sink as compared to the blowers.

In Figure 6, it is also clearly indicated that there is an optimization point for all four cases that have been investigated in this experiment. Because the optimization point varies between the heat sink geometries and fan types, it is concluded that both of the factors effect the heat sink optimization. In order to attain the optimum performance, the heat sink and system design, coupled with the fan selection is considered to be a critical path.

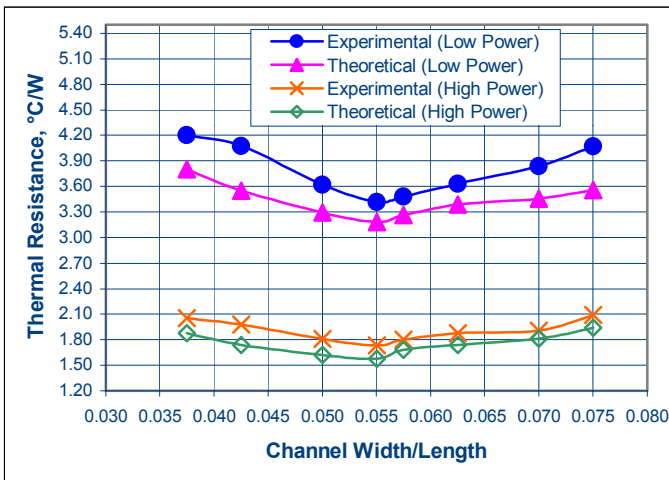


Figure 7. Total Thermal Resistance vs. The Channel Width/Length Ratio with Micro Blower

The blower theoretical and experimental thermal resistance is shown in Figure 7. Both of sets of data exhibit similar trends, and it is observed that the optimized point for both theoretical and experimental data agree. The theoretical data for the low

power blower shows an average of 9% better performance than the experimental data. The theoretical data for the high power blower showed an average of 8% better performance over the experimental data.

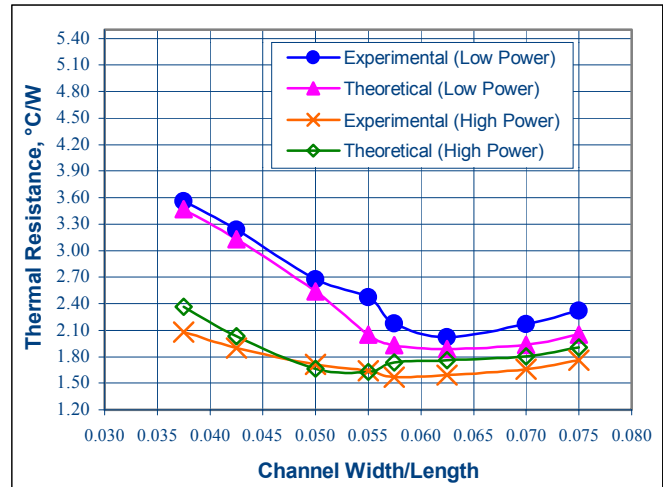


Figure 8. Total Thermal Resistance vs. The Channel Width/Length Ratio with Axial Fan

Figure 8 shows the comparison of thermal resistance and channel width/length ratio for the axial fans. In these cases, the experimental and theoretical for both axial fans exhibit the same trends. The theoretical and experimental optimization point for the high power axial fan did not match, however the optimization points identified were very close. As with the blowers, the theoretical axial fans outperformed the experimental results. The theoretical low power axial fan performed about 8% better and the theoretical high power axial fan performed about 6% better, compared with their corresponding experimental counterparts.

It is also noted that the theoretical data did find the experimental optimums in three of the four cases. This suggests that the methodology has the ability to determine the optimization point for the systems in the range tested. However, due to increased performance of the theoretical data, caution must be used if using the theoretical methodology to simulate the performance of a real world application. Future methodologies should also take into account minor resistances, such as fin to base bonding resistance, to build a more accurate picture of actual performance.

Conclusions

In this experiment, the primary goal was to characterize the performance of several fan-heat sink designs. In doing so, the optimization point can be found for the given space constraints. The thermal characterization and optimization points were found experimentally. The secondary goal was to find a theoretical methodology that would accurately predict both the optimization point for a given space as well as the performance of the solution. The chosen methodology did accurately predict the optimization point, however, it predicted better performance of the system on average by 6-10%.

References

- [1] Nelson, Daniel, "Enertron Inc. – Enertron's contribution the evolution of portable electronics cooling", *Electronics Cooling*, Vol. 6, Num. 1, pp. 8, January 2000.
- [2] Copeland, D., "Optimization of Parallel Plate Heatsinks for Forced Convection", *Proceedings of 16th IEEE Semiconductor Thermal Measurement & Management Symposium*, pp. 266-272, San Jose, CA, March 21-23, 2000.
- [3] Biber, C.R., and Fijol, S., "Fan-plus-Heatsink "Optimization" – Mechanical and Thermal Design with Reality", *Proceedings of the International Systems Packaging Symposium*, pp. 285-289, 1999.
- [4] Teertstra, P., Yovanovich, M.M., Culham, J.R., and Lemczyk, T., "Analytical Forced Convection Modeling of Plate Fin Heat Sinks", *Proceedings of 15th IEEE Semiconductor Thermal Measurement & Management Symposium*, pp. 34-41, San Diego, CA, March 9-11, 1999.
- [5] Bleier, P. Frank, *FAN HANDBOOK Selection, Application and Design*, 1st Edition, McGraw-Hill, New York, 1998.
- [6] Shah, R.K., and London, A.L., *Laminar Flow Forced Convection in Ducts*, Advances in Heat Transfer, Supplement 1, Academic Press, 1978.
- [7] Kays, William M., and London, A.L., "Analytic Solutions for Flow in Tubes", *Compact Heat Exchangers*, 3rd Edition, McGraw-Hill, New York, 1984.
- [8] Incropera, Frank P., and Dewitt, David P., "Internal Flow", *Fundamentals of Heat and Mass Transfer*, 4th Edition, John Wiley & Sons, New York, 1996.
- [9] Munson, Bruce R., Young, Donlad F., and Okiishi, Theodore H., *Fundamentals of Fluid Mechanics*, 2nd Edition, John Wiley & Sons, New York, 1994.
- [10] Loh, C.K., Chou, Bor-Bin, Nelson, Dan and Chou, D.J., "Thermal Behavior of Solder-Bonded and Adhesive Bonded Folded Fin Assemblies", *Proceedings of 16th IEEE Semiconductor Thermal Measurement & Management Symposium*, pp. 33-41, San Jose, CA, March 21-23, 2000.
- [11] Lee, Seri, "Calculating Spreading Resistance in Heat Sinks", *Electronics Cooling*, Vol. 4, Num. 1, pp. 30-33, January 1998.